Evaluation of the Estimation of the Applied Axial Tension Force in the Sagging Cables of the Kinh Duong Vuong Diagonal Arch Bridge in Vietnam

Ha Hoang
Faculty of Civil Engineering, University of Transport and Communications, Hanoi, Vietnam
hoangha@utc.edu.vn

Hung Dinh Nguyen
Faculty of Civil Engineering, Vietnamese-German University, Binh Duong, Vietnam
hung.nd2@vgu.edu.vn (corresponding author)

Received: 23 April 2025 | Revised: 16 May 2025 | Accepted: 31 May 2025

 DOI: https://doi.org/10.48084/etasr.11667

ABSTRACT

The Kinh Duong Vuong bridge is a diagonal arch bridge with a large arch height-to-span ratio. It was built using a combination of the balanced cantilever method and temporary piers for the deck, and a formwork system to fabricate the steel arches on the completed prestressed concrete decks. The Finite Element Method (FEM) was applied for the bridge design. Displacements of the arches and deck were recorded during its construction along with the tension forces in the cables. These values were then compared with the FEM results to confirm the bridge's load-bearing capacity. The indirect method of estimating the axial tension forces in the cables based on the vibration method was also evaluated. The modified effective length of the cables was determined by measuring the distance (from a point one cable diameter away from the hinge center to the internal damper at the cable end) using the anchorage. The results demonstrated that utilizing the modified effective length improved the accuracy of the indirect method for estimating the axial tension force in the cables.

Keywords-diagonal steel arch bridge; prestressed concrete deck; cable tension force; direct method; indirect method; vibration method; cable effective length

I. INTRODUCTION

Due to their aesthetics, arch bridges are typically used for long-span applications. Many spiral arch bridges have been constructed. Arch bridges can be classified into various types based on their materials and structural arrangements [1-6]. Modern arch bridges have a variety of configurations. One or more arch planes can be arranged in the transverse direction of the bridge. When arch planes are arranged at an angle to the bridge's longitudinal direction, a spatial arch bridge structure is formed. In a spatial arch bridge, the bridge deck is not connected to the arch(es). Therefore, the deck structure can only withstand vertical loads. Authors in [7] studied two cable hanger configurations of skew arch bridges. The results showed that the skew arch bridges have more advantages than the straight arch bridges under asymmetric loads. Many studies have been conducted on spiral arch bridges to determine their optimum response. The skew angle of the arches, which is defined as the angle between the longitudinal direction of the deck and the arch's axis in the plan, should range from 12° to 30° [7]. The arrangement of the cable hangers on a spiral arch bridge could increase its structural efficiency by limiting the clearance on the bridge surface. Authors in [4] explored the effect of the rotation angle of the arch and the angle of the cable to the plane of the arch on the inner forces on the arch and the deck. The results showed that the deck and arch were subjected to large horizontal loads. Authors in [8] analyzed the different variables and geometries of the spatial arch bridges to define them. Authors in [9] employed the influence matrix method to create a rapid design tool. Authors in [10] investigated the stability of a spiral arch bridge considering the effects of the main girder depth, rise-span ratio, and vertical ache arch rigidity using FEM. Authors in [11] deployed FEM to analyze the stability of a spiral arch bridge. Designing spatial arch bridge structures is very complex due to various parameters.

The Kinh Duong Vuong (KDV) bridge, an arch bridge with a unique spatial structure, was built over the Duong River in Bac Ninh Province, Vietnam. Due to its complex structure, the bridge required careful attention at both the design and construction stages. FEM was employed during the design

stage to analyze and optimize the bridge's structural components. During the tensioning of the cable, it was necessary to strictly control the elevation of the deck, the tension force in the cables. Also, it was required to monitor the deformation of the steel arches and prestressed concrete deck in both the vertical and transverse directions. These observations were then compared with the design values to confirm the bridge's load-bearing capacity.

Determining the tension force in the cable of a spiral arch bridge is important at the design, construction, and operation stages. A load cell is typically used to directly measure the tension force in the cable of a large-span bridge with long cables during construction and operation. However, this method is very expensive. For short cables, the tension force (T_0) is commonly measured using an indirect method based on the cable's vibration frequency. This method is considered simple, fast, and cost-effective. The tension force in a cable can be determined by the indirect method based on the cable's vibration frequency [12-24]. Nevertheless, the accuracy of the estimation equations remains a point of interest for civil engineers and researchers. The authors also took this opportunity to apply the indirect method to determine the tension force in the cables of the bridge. This could improve the accuracy of the indirect method and make it applicable to all types of cables in spatial arch bridges, cable-stayed bridges, and extradosed bridges, especially for load rating during service.

In this study, the KDV bridge was designed deploying FEM to determine the cable tension forces based on construction sequencing. The tension force in the cables was then directly determined using a pressure gauge on the jack and the cable's elongation was identified by controlling the elevation of the deck and the deflection of the arches in both the vertical and transverse directions. The tension force determined through the oscillation method was used to confirm the application of a modified equation for predicting the tension force in a cable using an indirect method.

II. MATERIALS AND METHODS

A. Main Structural Members of the KDV Bridge

The five main spans of the KDV Bridge were designed based on the diagonal arch bridge, as illustrated in Figure 1. The former were configured as 67.5+90+120+90+67.5 m. A prestressed concrete box girder of constant depth was chosen, as shown in Figure 2. Alternative geometries, such as parabolic, elliptical, and circular shapes can also be used. For this project, the arches were built with a semi-elliptical shape and were made of welded steel boxes with longitudinal and transverse stiffeners. The cross-section of the arches comprised isosceles trapezoids made up of 25 mm steel plates, as displayed in Figure 3. The cross-section depth of the steel arches for the spans of 67.5 m, 90 m, and 120 m was chosen as 3.0 m, 3.5 m, and 4.0 m, respectively. The toes of the steel arches are rigidly mounted on top of the piers. Therefore, the skew angles (θ) of the steel arches to the longitudinal axis of the bridge were different for each span. The skew angles in the spans of 67.5m, 90 m, and 120 m were 27°24', 21°15', and 16°16', respectively. These skew angles were in accordance with the specifications provided in [7].

The elliptical arch in each span was designed with a large height-to-span ratio to ensure an adequate clearance for vehicles passing through the bridge. The arch height-to-span length ratio in each span was selected to be 40/67.5, 51/90, and 67/120, respectively. Both the prestressed concrete deck girder and the steel arch were designed with high stiffness to resist large lateral and vertical loads. The distance between the anchorages for the cable hangers on the decks was chosen to be 6 m. Thus, the 67.5 m, 90 m, and 120 m prestressed concrete decks were supported by seven, eleven, and sixteen spiral prestressing cables of different areas, respectively, originating from the deck centerline. As portrayed in Figure 1, the cable hangers from the left to the right sides of spans 1 and 5, spans 2 and 4, and span 3 were named T_1 to T_7, T_1 to T_{11}, and T_1 to T_{16}, respectively.

B. Structural Modeling and Materials

FEM was used to model complex arch bridges [2-3, 26-27]. Figure 4 presents the KDV bridge model in RM 11 software. The reinforced concrete members, such as decks, piers, and piles, were modeled using the beam elements. The stiffness of the beam elements ($E_c \times I_{rc}$) was modified to account for the contribution of the steel rebars. The Young's modulus of concrete (E_c) was determined experimentally and was found to be 36.06 GPa. I_{rc} is the inertia of the reinforced concrete section. The unit weight of the reinforced concrete, 24.53 kN/m^3, is the average weight of the concrete and the normal reinforcement in a segment by volume. The passion ratio of the concrete was taken as 0.2. The compressive strength based on the cylinder test, f'_c, was approximately 45 MPa at 28 days. The behavior of the concrete in compression was based on the parabolic-rectangular stress–strain diagram, as specified in Eurocode 2 [28]. The tensile strength of concrete was neglected during the analysis.

The cable bundle type for hangers consists of 7 mm diameter Parallel Steel Wires (PWS), as specified in JSS II-11 [29]. The yield strength (f_{py}) of the cable at 8% elongation was 1370 MPa, and the Young's modulus (E) was tested to be 196 GPa. The internal tendons for the prestressed concrete were modeled using the TENDON element, and the cable hangers were modeled using the CABLE element. Tension force was introduced into the tendons and cables using the TENDON LOAD and CABLE techniques, respectively. A bilinear elasto-plastic constitutive model was appropriately modeled for both the prestressing tendons and cable hangers. The stiffness of the tendons and cables was expressed by $E \times A$, where A is the cross section of the tendon or cable. The steel plates for the arches conformed to ASTM A709 [30], with specified mechanical properties: yield strength (f_y) = 355 MPa, ultimate strength (f_u) = 610 MPa, and Young's modulus (E_s) = 200 GPa.

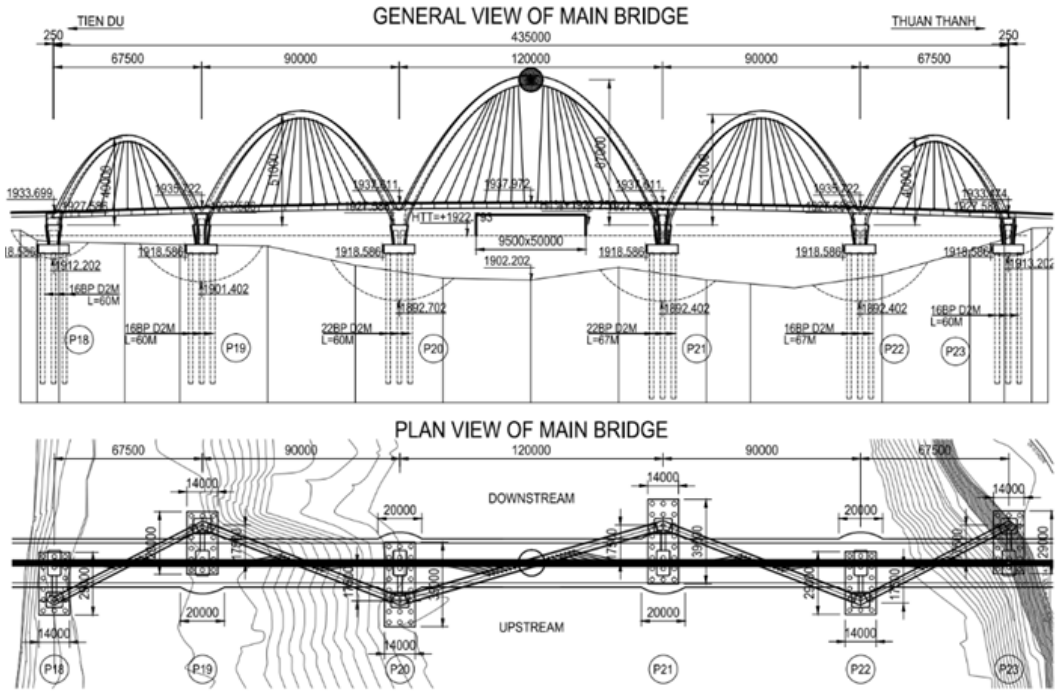

Fig. 1. Design of the five main spans of the KDV Bridge.

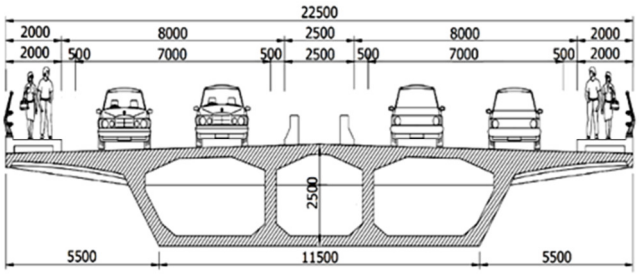

Fig. 2. Typical cross section of prestressed concrete beams.

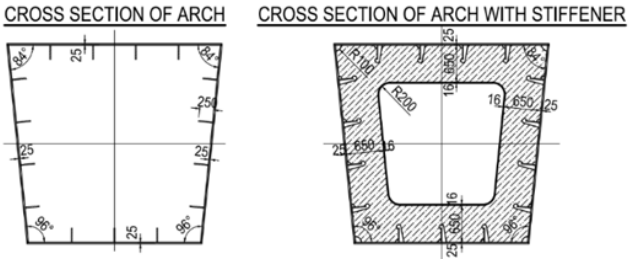

Fig. 3. Typical cross section of the arch.

The steel arches were also modeled using the BEAM element with a stiffness of $E_s \times I_{ar}$, where I_{ar} is the inertia of the arch cross section. The stress-strain relationship was defined using the ideal elastic model for the steel plate [25].

Based on the model analysis results, the cable tension forces were determined and subsequently used to calculate the required hanger cross-sectional areas. There are five types of cables used in the bridge, each with a different number of strands, designated as Types I, II, III, IV and V. The properties of the cables are listed in Table I. Figure 5 shows the arrangement of the cables for the middle span of L =120 m, with cable designations ranging from T_1 to T_{16} and cable types from I to V.

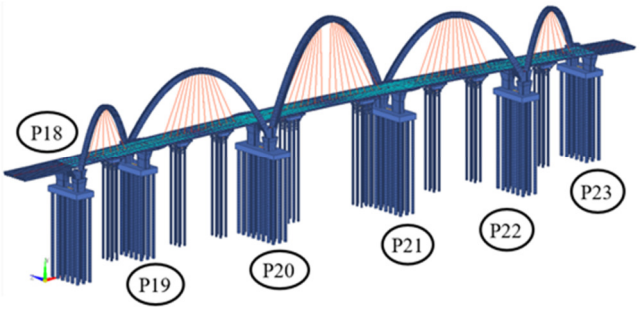

Fig. 4. The bridge model by RM version No. 11.

TABLE I. INFORMATION OF CABLES

Cable type	Type I	Type II	Type III	Type IV	Type V
Number of strands	61	73	91	109	139
Cross section area (mm^2)	2348	2809	3502	4195	5349
Moment of inertia (mm^4)	521350	1069069	1163407	2152336	358195
Ultimate force (kN)	4160	4970	6200	7420	9470
Unit weight (kg/m)	19.4	23.1	28.6	34.7	43.9
Total number of cables	12	14	14	10	2

The tension force on the cable was controlled according to the designed elevation of the bridge surface and the construction method. The tension force in the cables was applied in three stages. During the first stage, 50% of the designed tension force was applied to each cable to generate a vertical lifting force for the deck. After the first stage, all temporary pillars were released. In the second stage, the remaining 50% of the designed tension force was applied to the cables. Introducing a tension force to all cables simultaneously was impossible, therefore, a number of jacks was needed to perform this task. Ultimately, eight jacks were used to apply tension to eight cables at a time. Therefore, the tension force was applied eight times in both the first and second stages.

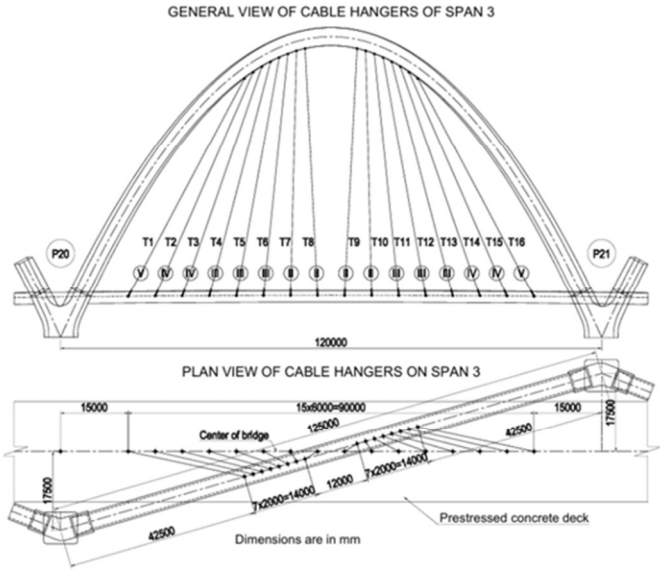

Fig. 5. Arrangements of tendons in the span of 120 m.

C. Tension Force in the Cables by the Direct Method

For this project, the prestressed concrete box girders were segmentally built by using the balanced cantilever method in combination with temporary piers. The steel arches were then fabricated using the steel scaffolding system supported on the bridge deck, as shown in Figure 6. Once the arching segments were connected, the arch scaffolding was removed. Next, the cables were installed to connect the steel arches to the deck system. Once the tension force was applied to the cables, the deck was lifted out of the temporary piers. A hydraulic jack applied the designed tension force simultaneously to all the wires in a cable, as depicted in Figure 7. Therefore, the tension force in each wire of a cable was nearly equal. The applied tension force and elongation of the cables were recorded. The actual tension force in the cables was calculated by:

$$T_r = T_d - (\Delta_L EA/l) \quad (1)$$

$$\Delta_L = \Delta_2 - \Delta_1 \quad (2)$$

where T_r represents the actual tension force in the cables (kN), T_d is the designed tension force applied to the cables (kN), which was recorded by the gauge of jack, Δ_L is the difference between the actual and designed elongations (mm), Δ_1 is the elongation of the cable due to the actual jacking force on the cable (mm), Δ_2 is the designed elongation of the cable due to the designed tension force (mm), E is the Young's modulus of the cable (MPa), A is the cross-section area of the cable (mm^2), and l is the designed length of the cable (mm), which is measured from the center of the hinge to the bearing plate of the anchorage.

Fig. 6. Construction of deck and arches.

Fig. 7. Controlling the tension force in cables by pressure and elongation gauges.

D. Measuring the Deformation of the Arches and Deck

The diagonal arches and deck were deformed in both the vertical and transverse directions at all times to introduce tension into the spatial cables. Figure 8 shows the resulting vertical and transverse displacements at monitored points on both the arches and deck. The monitored points were located at *L/2, L/4,* and *L/8* positions on each span [22]. The monitored points on the arches and bridge deck were labeled V_1 to V_{25} and D_1 to D_{25}, respectively.

E. Measuring the Natural Oscillation Frequency of Cables

Many researchers [12-24] have used the indirect method to determine the tension force in a cable, as illustrated in Figure 9. This method involves actively creating a forced oscillation in the cable using an external force. An acceleration transducer was attached to the cable hanger to measure its oscillating acceleration. The recorded acceleration value was converted to the cable's natural oscillation frequency using the Fast Fourier Transform (FFT) method. The vibration measurements of the cable hangers were taken using a Kyowa Q-953C acceleration transducer, as shown in Figure 9(b). The forced oscillation was generated by pulling the rope connected to the cable near its center with force, as depicted in Figure 9(c). The natural frequency of the cable was measured three times. The average values of the first, second, and third modes were utilized to estimate the tension force in the cable.

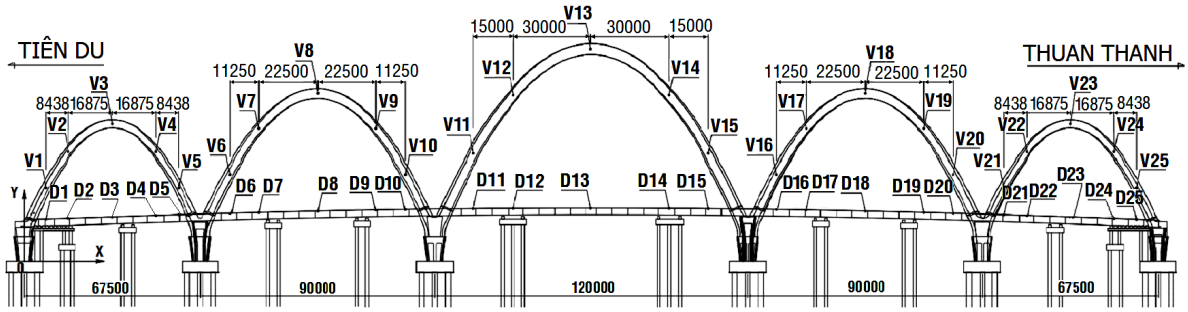

Fig. 8. Location of displacement transducers

(a) (b) (c)

Fig. 9. Measuring oscillation of cables: (a) data recording, (b) sensor installation, (c) force application.

III. DETERMINATION OF TENSION FORCE IN A CABLE THROUGH THE OSCILLATION METHOD

Figure 1 shows a sag-inclined cable in the x-y coordinates. The flexural stiffness ($E \times I$) and tension force (T) of the entire cable are assumed to be constant. The motion in the y-direction of the cable can be expressed as [31]:

$$EI\frac{\partial^4 v(x,t)}{\partial x^4} - T\frac{\partial^2 v(x,t)}{\partial x^2} - h(t)\frac{\partial^4 y}{\partial x^2} + \frac{w}{g}\frac{\partial^2 v(x,t)}{\partial t^2} = 0 \quad (3)$$

where $v(x,t)$ is the deflection in the y-direction due to vibration, $h(t)$ is the derivative cable force caused by vibration, w is the unit weight of the cable, and g is the gravitational acceleration (9.81 m/s^2). If $v(x,t)$ is very small and the cable deformation is the parabolic line, (3) can be rewritten as:

$$EI\frac{\partial^4 v(x,t)}{\partial x^4} - T\frac{\partial^2 v(x,t)}{\partial x^2} + \frac{w}{g}\frac{\partial^2 v(x,t)}{\partial t^2} = \frac{8d}{l^2}h(t) \quad (4)$$

For a higher order mode, $h(t)$ has a very small effect, therefore, (4) is approximated as:

$$EI\frac{\partial^4 v(x,t)}{\partial x^4} - T\frac{\partial^2 v(x,t)}{\partial x^2} + \frac{w}{g}\frac{\partial^2 v(x,t)}{\partial t^2} = 0 \quad (5)$$

Authors in [13] solved (5) with some approximate parameters, which are given in the following forms.

- For the cables with a sufficiently small sag ($3 \le \Gamma$), the first-order natural frequency was used:

$$T = \frac{4w(f_1 l)^2}{g}\left[1 - 2.2\frac{C}{f_1} - 0.55\left(\frac{C}{f_1}\right)^2\right] \text{ for } 17 \le \xi \quad (6)$$

$$T = \frac{4w(f_1 l)^2}{g}\left[0.865 - 11.6\left(\frac{C}{f_1}\right)^2\right] \text{ for } 6 \le \xi \le 17 \quad (7)$$

$$T = \frac{4w(f_1 l)^2}{g}\left[0.828 - 10.5\left(\frac{C}{f_1}\right)^2\right] \text{ for } 0 \le \xi \le 6 \quad (8)$$

- For cables with a relatively large sag ($\Gamma \le 3$), the second-order natural frequency was utilized:

$$T = \frac{4w(f_2 l)^2}{g}\left[1 - 4.4\frac{C}{f_2} - 1.1\left(\frac{C}{f_2}\right)^2\right] \text{ for } 60 \le \xi \quad (9)$$

$$T = \frac{4w(f_2 l)^2}{g}\left[1.03 - 6.33\frac{C}{f_2} - 1.58\left(\frac{C}{f_2}\right)^2\right]$$

$$\text{for } 17 \le \xi \le 60 \quad (10)$$

$$T = \frac{4w(f_2 l)^2}{g}\left[0.882 - 85\left(\frac{C}{f_2}\right)^2\right] \text{ for } 0 \le \xi \le 17 \quad (11)$$

- For very long cables where higher-order modes dominate ($n > 2$), the natural frequencies of these modes were utilized:

$$T = \frac{4w(f_n l)^2}{n^2 g}\left[1 - 2.2\frac{nC}{f_n}\right] \quad \text{for } 200 \le \xi \quad (12)$$

where ξ, C, and Γ are non-dimensional parameters calculated using:

$$\xi = \sqrt{\frac{T}{EI}}\,l \quad (13)$$

$$C = \sqrt{\frac{EIg}{wl^4}} \quad (14)$$

$$\Gamma = \sqrt{\frac{wl}{128EA\delta^3 cos^5\theta}} \frac{0.31\xi+0.5}{0.31\xi-0.5} \quad (15)$$

In the case of a straight cable or cables in which the effect of the sag was ignored, the tension force (T) in the cable can be calculated using:

$$T = \frac{4w(fl)^2}{g} \quad (16)$$

where I is the moment of inertia of the cable, δ is the sag-to-span ratio of the cable ($\delta = s/\ell_0$), y is displacement in the y direction, θ is the inclination angle of the cable (deg.), and f_i is the natural frequency of the cable corresponding to mode order (H_z).

Regarding the inclined cable model, the solutions of [13] were applied to the wire between the two hinges. This could be considered as a hinged-hinged model. However, the inclined cables were connected to the beam and arch via an anchorage and/or a hinge which could be considered a fixed-hinged cable or fixed-fixed cable. The designed length of the cable could not be used to estimate its natural frequency. To estimate a cable's natural frequency, its designed length must account for the effects of the hinge connection, the anchorage length, and the damping device (if applicable). To increase the accuracy, authors in [17] reduced the designed cable length by a value equal to its diameter. Meanwhile, authors in [18] considered the effect of the bending stiffness on the fixed-fixed and fixed-hinged boundaries. The accuracy of the in [13, 17-18] was also evaluated based on the comparison with the direct tension force in the KDV bridge cables.

IV. RESULTS AND DISCUSSION

The designed cable tension forces (T_d) and their application sequence, as determined by FEM, are provided in Appendix 1. In each row of Appendix 1, the number in the shaded cell represents the tension force that was directly applied to the cable. The remaining values indicate the residual tension forces in the cables after tensioning other cables in subsequent steps. All cables are under tension under all types of loads. Figure 10 presents the FEM-calculated response to cable tensioning, showing deck bending moments, stresses in upstream/downstream top/bottom fibers of prestressed concrete decks, and vertical deformations of decks and arches. The FEM model analysis results satisfied the design criteria.

The total station was used to collect the vertically measured displacements of the arches and deck when the actual tension force was applied to the cables. These results were then compared with those from FEM. Figure 11 illustrates the vertically designed and measured displacements of the arches and decks at the first and second stage of tensioning. After the completion the second-stage, the third-stage was carried out to adjust the bridge surface to the designed level. The displacements of the steel arches and prestressed concrete decks at the measured points after the third-stage are presented in Figure 12. The absolute deviation between the designed and measured values of the arches in the longitudinal, transverse, and vertical directions was 9 mm, 10 mm, and 15 mm, respectively. Meanwhile, the absolute deviation between the designed and measured values of the deck in the transverse and vertical directions was 5 mm and 33 mm, respectively. These deviations were small compared to the span length of the structures. Such deviations are common in bridge constructions because the actual stiffness of prestressed concrete decks and steel arches is often greater than the theoretical value. Stiffer structures could result from larger structural dimensions due to manufacturing errors, a higher elastic modulus of concrete than the designed value, and ignoring the effect of normal reinforcing steel. The actual tension force in the cables at the third-stage of stretching the cables (T_0) was calculated and listed in Appendix 2. The results showed that the maximum, mean, and minimum values of T_d/T_0 ratios and the standard deviation were 1.30, 1.03, 0.83, and 0.13, respectively. Based on the comparison of the elevation of the deck, the deflection of the arches, and the tension force in the cables, the construction technique for the KDV bridge fulfilled the technical requirements based on the FEM results.

A. Evaluating the Tension Force in the Cable by the Oscillation Method

Figure 13 displays the natural oscillation frequency chart of some cable hangers recorded through acceleration measurement. The oscillation frequency of the cables is demonstrated in Appendix 2 based on the FFT analysis. To determine the T value from (6-12), the values of $\hat{\imath}$, C, and Γ from (13-15) must be calculated. The values of $\hat{\imath}$, C, and Γ depend on many parameters such as T, l, E, I, A, δ, and θ, which are also listed in Appendix 2. If there were no information about the axial force in a cable, the T value from (16) would be used to predict the $\hat{\imath}$ value from (13). The iterative calculation method was then conducted. The actual tension force in the cables (T_0) was obtained from the direct method by using hydraulic jacks. This is a consistent and reliable method to obtain tension force. The tension force (T_0) value was then used to calculate the $\hat{\imath}$ value from (13). The calculated values of $\hat{\imath}$, C, and Γ are also given in Appendix 2. Almost all Γ values were greater than 3. The value of Γ in some cables was less than 3. These were cables near the ends of each span, which had a small inclined angle and large deflection. The static shape of the sag-inclined cables, expressed by the sag-to-span ratio (δ), is often not easy to measure with high accuracy [15], especially for vibrating cables.

All values of $\hat{\imath}$ are greater than 60. The T value can be determined by (6), (9), and (12) in which the design length (l) of cables was used to calculate the axial tension force in cables (T_1). The design length (l) of the cables was needed to consider the effect of the bridge surface and the deformed arch after construction. The calculated T_1 values from (9) (for cables with $\Gamma < 3$) and from (12) exhibited significant deviations from the reference tension T_0. However, the calculated T_1, value using (6) (for cables with $\Gamma < 3$) were close to the T_0 value, as shown in Appendix 3. This suggests that all cables acted as short cables with the first-order vibration mode.

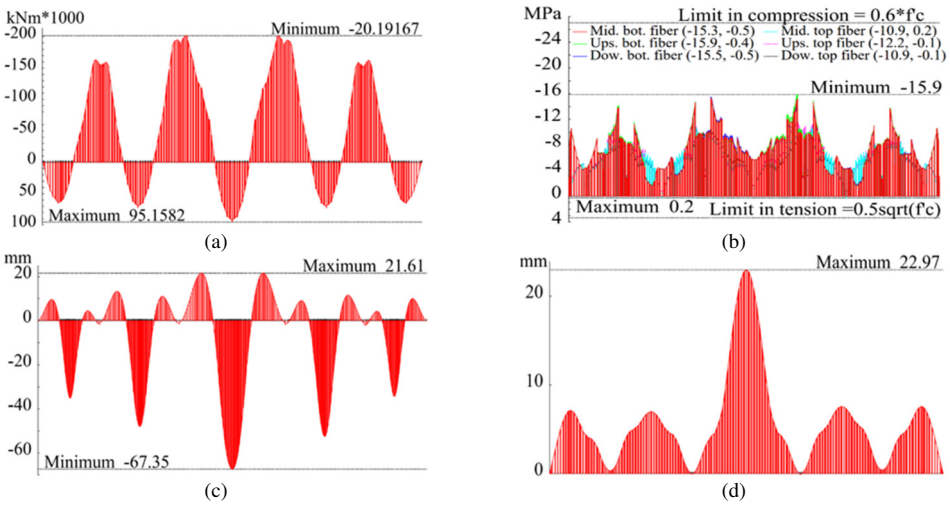

Fig. 10. Performance of the bridge structures during cable stretching: (a) moment in deck at prestressing at the first-time of the first-stage, (b) stress in the uppermost and lowermost fibers of the deck, (c) vertical deformation of deck at prestressing at the second-time of the second-stage, (d) vertical deformation of arches at prestressing at the eighth-time of second-stage.

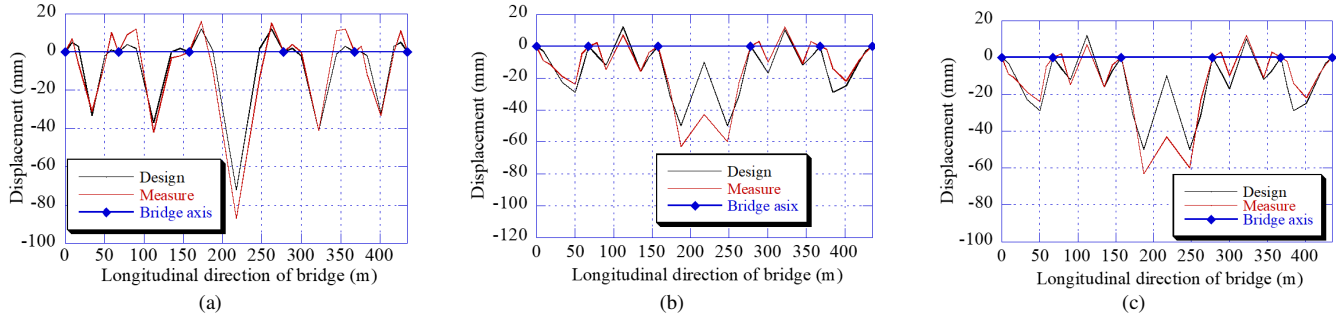

Fig. 11. Designed and measured displacements of arches and decks at first and second stages: (a) arch displacement at the eighth-time of the second-stage, (b) deck displacement at the first-time of the first-stage, (c) deck displacement at the eighth-time of the second-stage.

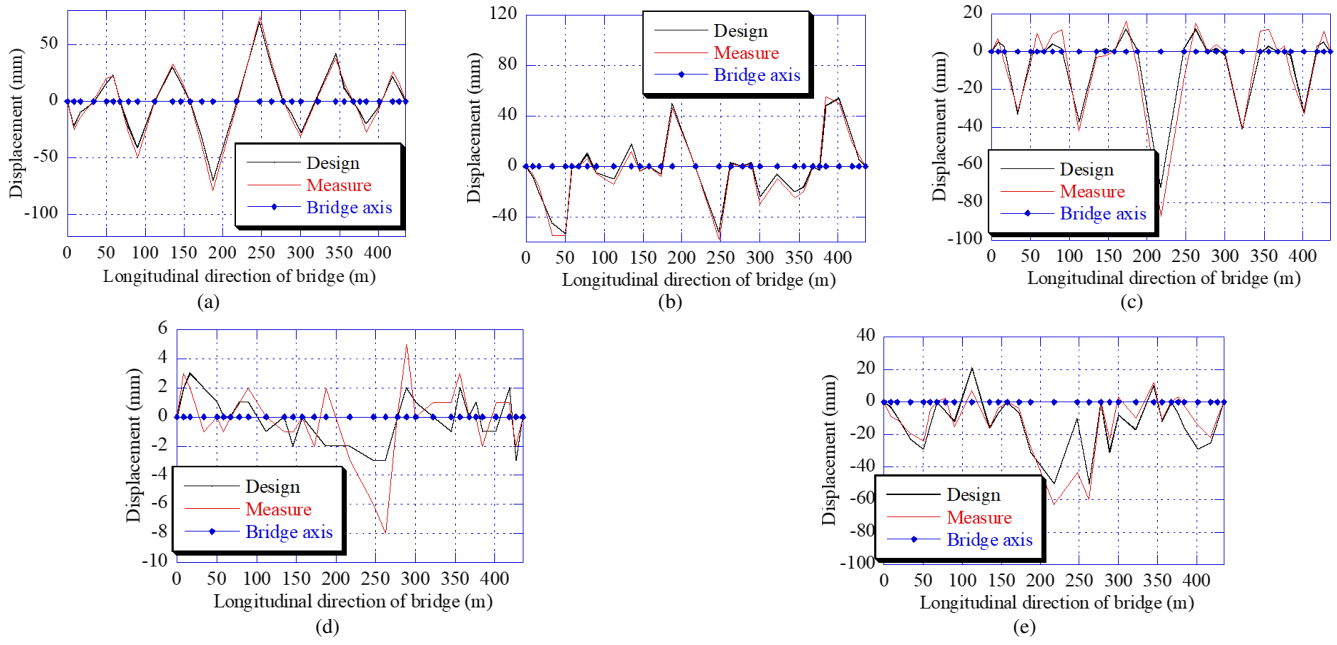

Fig. 12. Designed and measured displacements of arches and deck at step 3: (a) longitudinal direction of arches, (b) transverse direction of arches, (c) vertical direction of arches, (d) transverse direction of deck, (e) vertical direction of deck.

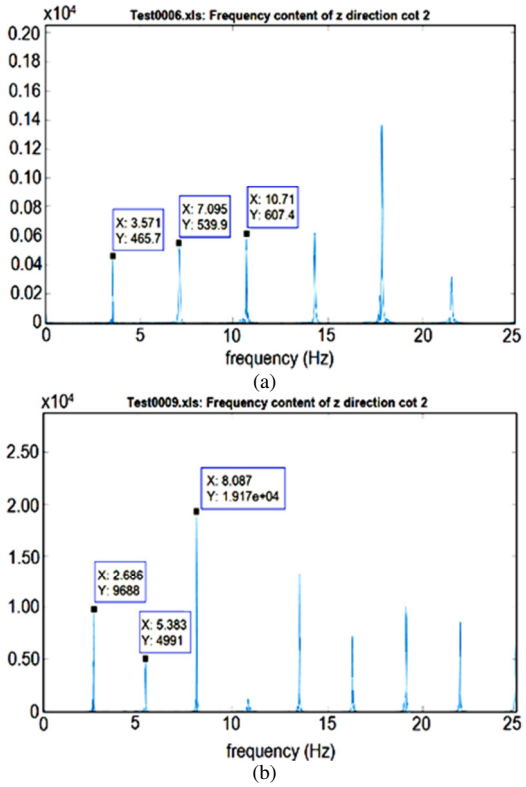

Fig. 13. Natural frequency of span 2: (a) cable T1, (b) cable T5.

Equation (6) was used to evaluate the accuracy of the calculated axial tension force in the cables. The mean value of T_1/T_0 is 1.071, while the maximum and minimum T_1/T_0 ratios are 1.261 and 0.939, respectively. Meanwhile, the standard deviation is 0.054. Using the design length to determine the axial tension force in the cables resulted in a 7.1% error in the mean value.

The previous equations [13, 17-18] are able to reduce the accuracy of estimating the tension force in the cables of the KDV bridge. In this project, the inclined cables were connected to the beam and arch via an anchorage and a hinge, as shown in Figure 14. The hinge can rotate freely. The cables in the KDV bridge can be considered a fixed-hinged cable model. Meanwhile, the solutions of [13] were applied to the hinged-hinged cable model. Additionally, authors in [13] used the design length of the cable for estimation. However, for the vibrating inclined cables, the design length was not suitable because the cable could not rotate at the anchorage bearing point. This could cause inaccuracy in the solutions of [13]. The design length is suitable for the static structural design. Therefore, the design length of the cable should be considered to determine the axial tension force in the cable. The axial tension forces in the cables were calculated based on the methods given in [17-18]. These forces are presented in the T_2 and T_3 in Appendix 3, respectively. The maximum, mean, and minimum values of the T_2/T_0 ratios and the standard deviation were 1.255, 1.067, 0.935, and 0.053, respectively. Meanwhile, the maximum, mean, and minimum values of the T_3/T_0 ratios and the standard deviation were 1.228, 1.041, 0.904, and 0.266, respectively. The error of the estimated mean value of the axial tension force in the cables, provided in [17], was 6.7%. This improvement was minimal compared to that of [13] regarding the design length. The results of [18] revealed a better mean value compared to that of [17]. However, the standard deviation from the method deployed in [18] was much larger than that from the method utilized in [17].

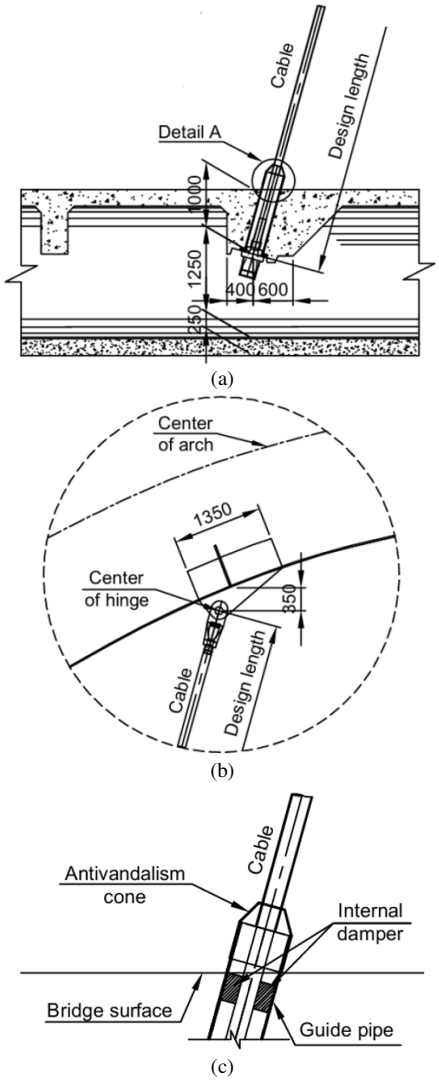

Fig. 14. A typical cable: (a) fixed anchorage, (b) hinge, (c) detail of section A.

For the fixed anchorage, the internal damper was located approximately 1.0 m away from the bearing plate and close to the deck surface, as illustrated in Figure 14(c). The modified effective length of the cables, which was used to determine the axial force via the indirect method, was, therefore, determined by measuring the distance from a point located one cable diameter away from the hinge center to the internal damper at the cable end, using the anchorage as in (17). Following the approach proposed in [17], the cable diameter was reduced along its effective length to account for the hinge effects, as illustrated in Figure 14(b).

$$l_e = l - l_p - d_c \quad (17)$$

where l_e is the modified effective length of the cable (m), l is the design length, l_p is the length from the bearing plate to the internal damper (m), and d_c is the diameter of the cable (m). The solutions of [13] using l_e for (6) are shown in T_4. The results demonstrate that the maximum, mean, and minimum values of the T_4/T_0 ratios and the standard deviation according to the proposed method are 1.194, 1.015, 0,875, and 0.054, respectively. These results demonstrate greater accuracy compared to the findings of the methods using the design length (l) [13] and the approaches proposed in [17-18], as evidenced in Figure 15. The estimated minimum ratio is smaller than that of other methods. This can affect the durability of the cables. The estimated T_4/T_0 ratios for the three cables deviate by more than 10%. The cable stress was designed at 50% of the yield strength to maintain an adequate safety margin. Therefore, there are sufficient durability reserves in all cables. Using the l_e value from [18] could not improve the estimated axial tension force in the cable.

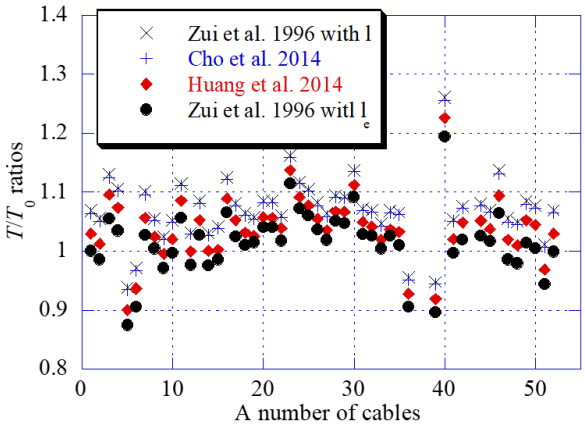

Fig. 15. Accuracy of different methods.

V. CONCLUSIONS

The diagonal arch bridge is complex in terms of both design and construction. Therefore, the diagonal arch bridge required appropriate technological solutions regarding its design and construction. Based on the performed analysis and evaluation, the following conclusions are drawn:

- The combination of the balanced cantilever method and temporary piers was an appropriate technical solution for the construction of the arched bridge crossing a large river.
- In the bridge design, using the Finite Element Method (FEM) to build a 3D model to simulate the main structures and temporary substructures of the bridge, gave a highly accurate and reliable result.
- The method utilized in [13] demonstrated higher accuracy in predicting the tension force through the vibration method, assuming an ideal hinged-hinged cable model. When this method is applied to practical bridges, it is necessary to consider the effective length of the cable hanger to increase the accuracy.
- The indirect method for determining the axial tension force in the cables considering the effective cable length of cables from this paper was an effective technical solution that could be widely applied to all types of cables in spatial arch bridges, cable-stayed bridges, and extradosed bridges, especially during the service time of the bridge.

ACKNOWLEDGMENTS

This research is funded and supported by the Bac Ninh Department of Transport for the survey and experimental activities in the field. This support is gratefully acknowledged.

REFERENCES

[1] F. T. K. Au, J. J. Wang, and G. D. Liu, "Construction Control of Reinforced Concrete Arch Bridges," *Journal of Bridge Engineering*, vol. 8, no. 1, pp. 39–45, Jan. 2003, https://doi.org/10.1061/(ASCE)1084-0702(2003)8:1(39).

[2] D. Yu-wen and W. You-yuan, "A Research to Cable Force Optimizing Calculation of Cablestayed Arch Bridge," *Procedia Engineering*, vol. 37, pp. 155–160, 2012, https://doi.org/10.1016/j.proeng.2012.04.219.

[3] S. Farahmand-Tabar and M. Barghian, "Response control of cable-stayed arch bridge using modified hanger system," *Journal of Vibration and Control*, vol. 26, no. 23–24, pp. 2316–2328, Dec. 2020, https://doi.org/10.1177/1077546320921635.

[4] J. Aguilar-Jiménez, J. M. García-Guerrero, and J. J. Jorquera-Lucerga, "The Diagonal Arch Bridge, a Particular Case of Spatial Arch Bridges," *Applied Sciences*, vol. 11, no. 4, Feb. 2021, Art. no. 1869, https://doi.org/10.3390/app11041869.

[5] H. Wang, L. Wang, X. Zhuo, K. Huang, X. Wang, and W. Wang, "Study on the Precise Displacement Controlling Method for a Suspended Deck in the Hanger Replacement Process of an Arch Bridge," *Applied Sciences*, vol. 11, no. 20, Oct. 2021, Art. no. 9607, https://doi.org/10.3390/app11209607.

[6] L. Todisco, H. Corres, A. Pérez, A. Addante, and J. Cañada, "Conceptual design of spatial arch footbridges supporting curved decks," *Structures*, vol. 33, pp. 1207–1215, Oct. 2021, https://doi.org/10.1016/j.istruc.2021.05.003.

[7] P. Walle, "Skew Placement of Arches for Single Span Road Bridges," Master's Thesis, Ghent University, Ghent. Belgium, 2017.

[8] M. Sarmiento-Comesías, A. M. Ruiz-Teran, and A. C. Aparicio, "State-of-the-art of spatial arch bridges," *Proceedings of the Institution of Civil Engineers - Bridge Engineering*, vol. 166, no. 3, pp. 163–176, Sep. 2013, https://doi.org/10.1680/bren.11.00010.

[9] M. Modano, A. Majumder, F. Santos, R. Luciano, and F. Fraternali, "Fast and Optimized Calculation of the Cable Pretension Forces in Arch Bridges with Suspended Deck," *Frontiers in Built Environment*, vol. 6, Jul. 2020, Art. no. 114, https://doi.org/10.3389/fbuil.2020.00114.

[10] W. L. Qui, C. S. Kao, C. H. Kuo, J. L. Tsai, and G. Yang, "Stability Analysis of Special-Shape Arch Bridge," *Journal of Applied Science and Engineering*, vol. 13, no. 4, pp. 365–373, 2010.

[11] X. Peng, X. N. Wang, and X. Gui, "3D Finite Element Analysis of Single Span Special-Shape Arch Bridge with Diagonal Crossing Arch Rib and Curved Girder," *Applied Mechanics and Materials*, vol. 63–64, pp. 915–918, Jun. 2011, https://doi.org/10.4028/www.scientific.net/AMM.63-64.915.

[12] J. R. Casas, "A Combined Method for Measuring Cable Forces: The Cable-Stayed Alamillo Bridge, Spain," *Structural Engineering International*, vol. 4, no. 4, pp. 235–240, Nov. 1994, https://doi.org/10.2749/101686694780601700.

[13] H. Zui, T. Shinke, and Y. Namita, "Practical Formulas for Estimation of Cable Tension by Vibration Method," *Journal of Structural Engineering*, vol. 122, no. 6, pp. 651–656, Jun. 1996, https://doi.org/10.1061/(ASCE)0733-9445(1996)122:6(651).

[14] A. Eklund, "Measurement and Evaluation of Cable Forces in the Alvsborg Bridge," Master's Thesis, Royal Institute of Technology, Stockholm, Sweden, 2006.

[15] B. H. Kim, T. Park, H. Shin, and Yoon, "A Comparative Study of the Tension Estimation Methods for Cable Supported Bridges," *International Journal of Steel Structures*, vol. 7, pp. 77–84, 2007.

[16] Z. Fang and J. Wang, "Practical Formula for Cable Tension Estimation by Vibration Method," *Journal of Bridge Engineering*, vol. 17, no. 1, pp. 161–164, Jan. 2012, https://doi.org/10.1061/(ASCE)BE.1943-5592.0000200.

[17] Cho, Soojin, Yun, Chung-bang, and Sim, Sung-Han, "Evaluation of Cable Tension Forces Using Vibration Method for a Cable-stayed Bridge under Construction," *Journal of the Korean Society of Safety*, vol. 29, no. 2, pp. 38–44, Apr. 2014, https://doi.org/10.14346/JKOSOS.2014.29.2.038.

[18] Y.-H. Huang, J.-Y. Fu, R.-H. Wang, Q. Gan, and A.-R. Liu, "Unified Practical Formulas for Vibration-Based Method of Cable Tension Estimation," *Advances in Structural Engineering*, vol. 18, no. 3, pp. 405–422, Mar. 2015, https://doi.org/10.1260/1369-4332.18.3.405.

[19] P. Jakiel and Z. Mańko, "Estimation of cables' tension of cable-stayed footbridge using measured natural frequencies," *MATEC Web of Conferences*, vol. 107, 2017, Art. no. 00006, https://doi.org/10.1051/matecconf/201710700006.

[20] Z. Huang and X. Zhang, "Research on Practical Determination of Cable Tension," *Asian Journal of Applied Sciences*, vol. 5, no. 5, pp. 922–926, 2017.

[21] A. Furukawa, K. Hirose, and R. Kobayashi, "Tension Estimation Method for Cable with Damper Using Natural Frequencies," *Frontiers in Built Environment*, vol. 7, Apr. 2021, Art. no. 603857, https://doi.org/10.3389/fbuil.2021.603857.

[22] Y. Xu, J. Zhang, Y. Zhang, and C. Li, "A Novel Approach for Cable Tension Monitoring Based on Mode Shape Identification," *Sensors*, vol. 22, no. 24, Dec. 2022, Art. no. 9975, https://doi.org/10.3390/s22249975.

[23] W. Zhang and Z. Wang, "Frequency-Based Cable Tension Identification Using a Nonlinear Model with Complex Boundary Constraints," *Shock and Vibration*, vol. 2023, pp. 1–19, Feb. 2023, https://doi.org/10.1155/2023/7795452.

[24] M.-H. Nguyen, T.-D.-N. Truong, T.-C. Le, and D.-D. Ho, "Identification of Tension Force in Cable Structures Using Vibration-Based and Impedance-Based Methods in Parallel," *Buildings*, vol. 13, no. 8, Aug. 2023, Art. no. 2079, https://doi.org/10.3390/buildings13082079.

[25] T. H. Nguyen, "Global Sensitivity Analysis of In-Plane Elastic Buckling of Steel Arches," *Engineering, Technology & Applied Science Research*, vol. 10, no. 6, pp. 6476–6480, Dec. 2020, https://doi.org/10.48084/etasr.3833.

[26] J. C. Wilson and W. Gravelle, "Modelling of a cable-stayed bridge for dynamic analysis," *Earthquake Engineering & Structural Dynamics*, vol. 20, no. 8, pp. 707–721, Jan. 1991, https://doi.org/10.1002/eqe.4290200802.

[27] Z. Liu, S. Zhou, K. Zou, and Y. Qu, "A numerical analysis of buckle cable force of concrete arch bridge based on stress balance method," *Scientific Reports*, vol. 12, no. 1, Jul. 2022, Art. no. 12451, https://doi.org/10.1038/s41598-022-15755-w.

[28] Eurocode 2: Design of Concrete Structures—Part I: General Rules and Rules for Buildings, EN 1992-1-1, European Committee for Standardization, Brussels, Belgium, 2018.

[29] *Parallel wire cable*, JSS II-11, Japanese Society of Steel Construction, Japan, 1994.

[30] *Specification for Structural Steel for Bridges*, ASTM A709/A709M-21, ASTM International, Pennsylvania, USA, 2021.

[31] T. Shimada, "Estimating method of cable tension from natural frequency of high mode," in *Proceedings of the Japan Society of Civil Engineers*, Japan, 1994, vol. 1, pp. 163–171.

APPENDIX 1. APPLIED TENSION FORCE FOR CABLES BASED ON DESIGN

Span	Cable	Series of tensioning application for the 1st stage (kN)								Series of tensioning application for the 2nd stage (kN)							
		1st time	2nd time	3rd time	4th time	5th time	6th time	7th time	8th time	1st time	2nd time	3rd time	4th time	5th time	6th time	7th time	8th time
span 1	T1							1701	1701	1894	1906	1895	1862	1798	1708	2150	2150
	T2						1400	1206	1206	1409	1408	1387	1351	1293	1851	1786	1786
	T3					1301	1195	1077	1077	1277	1266	1239	1202	1751	1696	1653	1653
	T4				1250	1186	1124	1065	1065	1277	1255	1219	1701	1661	1622	1593	1593
	T5			1348	1293	1255	1235	1234	1234	1459	1422	1950	1913	1883	1859	1847	1847
	T6		1696	1598	1548	1541	1570	1639	1639	1842	2299	2244	2211	2195	2192	2199	2199
	T7	2194	1947	1829	1790	1819	1905	2056	2056	2797	2732	2677	2653	2656	2679	2712	2712
Span 2	T1	2504	2377	2283	2226	2182	2164	2168	2179	3158	3086	3032	2975	2910	2874	2877	2877
	T2		1903	1811	1752	1707	1689	1682	1694	1614	2504	2441	2370	2285	2238	2241	2241
	T3			1502	1458	1424	1410	1412	1413	1341	1289	1970	1913	1841	1801	1803	1803
	T4				1002	952	931	934	936	832	770	708	1374	1271	1212	1214	1215
	T5					801	775	778	779	675	611	544	454	1174	1104	1106	1107
	T6						800	803	804	714	651	583	490	363	1249	1252	1253
	T7					901	875	878	879	812	751	684	595	1352	1282	1285	1286
	T8				1101	1056	1037	1040	1041	1003	952	897	1573	1482	1430	1432	1433
	T9			1491	1429	1380	1361	1365	1367	1338	1276	1928	1852	1757	1705	1707	1708
	T10		1902	1809	1745	1698	1680	1684	1686	1667	2508	2448	2380	2298	2253	2256	2257
	T11	2503	2370	2276	2212	2166	2150	2154	2157	3159	3099	3050	2997	2936	2903	2905	2907
span 3	T1	2700	2569	2455	2374	2306	2250	2209	2177	3849	3780	3736	3704	3679	3656	3636	3621
	T2		2100	2004	1934	1873	1824	1786	1757	2023	3099	3053	3016	2983	2951	2921	2899
	T3			2000	1920	1848	1786	1737	1698	2167	2100	2858	2799	2751	2701	2654	2617
	T4				1600	1525	1457	1401	1356	1895	1839	1787	2400	2347	2288	2232	2188
	T5					1500	1409	1331	1266	1908	1855	1800	1742	2301	2226	2153	2094
	T6						1350	1244	1155	1857	1807	1752	1691	1618	2151	2062	1998
	T7							1150	1059	1643	1605	1563	1512	1451	1374	1851	1782
	T8								1000	1585	1549	1507	1458	1395	1316	1231	1600
	T9								1000	1585	1549	1507	1457	1395	1315	1230	1600
	T10							1150	1059	1642	1604	1561	1511	1450	1372	1849	1781
	T11						1350	1244	1155	1855	1804	1750	1689	1616	2149	2060	1997
	T12					1500	1409	1331	1266	1906	1853	1798	1740	2299	2224	2151	2092
	T13				1600	1525	1457	1401	1356	1894	1838	1786	2400	2346	2287	2232	2187
	T14			2000	1920	1848	1785	1736	1697	2168	2100	2850	2799	2752	2702	2655	2618

	T15		2100	2003	1933	1873	1823	1785	1756	2024	3101	3054	3017	2985	2952	2923	2900
	T16	2700	2567	2454	2373	2304	2248	2207	2175	3853	3782	3737	3705	3680	3657	3637	3622
span 4	T1	2497	2359	2259	2192	2144	2128	2135	2137	3141	3077	3025	2969	2904	2870	2872	2874
	T2		1898	1799	1731	1682	1665	1670	1673	1653	2492	2429	2359	2273	2226	2229	2231
	T3			1509	1460	1422	1408	1412	1413	1393	1345	2011	1953	1880	1840	1842	1843
	T4				1099	1051	1033	1037	1038	1002	949	893	1567	1473	1420	1423	1424
	T5					899	872	877	878	816	753	685	594	1348	1278	1280	1281
	T6						800	804	806	723	659	589	495	366	1251	1253	1254
	T7					799	772	777	778	683	618	550	459	1176	1106	1108	1109
	T8				998	947	926	931	932	838	775	712	1376	1272	1231	1215	1216
	T9			1498	1453	1417	1403	1407	1408	1341	1289	1969	1911	1839	1798	1800	1801
	T10		1897	1800	1739	1692	1675	1680	1682	1607	2496	2432	2360	2274	2226	2229	2230
	T11	2496	2363	2265	2206	2161	2144	2151	2152	3142	3068	3014	2956	2890	2854	2857	2857
span 5	T1	2202	1953	1837	1799	1828	1911	2058	2058	2803	2741	2686	2644	2667	2690	2722	2722
	T2		1701	1601	1552	1544	1570	1635	1636	1843	2301	2247	2215	2200	2197	2203	2203
	T3			1351	1294	1255	1232	1228	1228	1457	1421	1950	1913	1884	1860	1847	1847
	T4				1250	1184	1120	1057	1057	1273	1252	1216	1699	1659	1620	1591	1591
	T5					1299	1191	1070	1070	1273	1263	1236	1200	1749	1694	1650	1650
	T6						1399	1200	1200	1406	1406	1385	1350	1292	1849	1784	1783
	T7							1698	1698	1894	1907	1896	1863	1799	1709	2150	2150

APPENDIX 2. SOME PARAMETERS AND RESULTS

Span	Cable	T_0 (kN)	f_1 (Hz)	l (m)	d (m)	θ (deg)	δ	Γ	ξ	C
Span 1	T1	2056.4	4.105	34.474	0.077	65°48'	0.0076	4.8	101.13	0.08
	T2	1665.6	4.227	33.391	0.081	73°19'	0.005	17.8	92.26	0.09
	T3	1451	4.532	32.615	0.092	80°58'	0.0028	152.6	120.35	0.07
	T4	1598.7	4.7	32.131	0.081	90°00'	0	∞	124.46	0.07
	T5	2014.7	4.547	32.202	0.081	80°39'	0.0024	217.4	97.79	0.10
	T6	2662.1	4.701	32.634	0.077	72°21'	0.0042	24.1	109.24	0.09
	T7	3267	4.929	33.411	0.068	66°35'	0.0053	10.8	90.79	0.10
Span 2	T1	3181.5	3.571	44.349	0.077	61°50'	0.0132	**1.8**	119.60	0.06
	T2	2269.7	3.357	43.152	0.081	67°20'	0.0141	**2.3**	134.04	0.05
	T3	1875.6	3.525	42.18	0.077	72°21'	0.0083	8.8	124.22	0.06
	T4	1180.2	3.189	41.44	0.081	78°18'	0.0069	26.4	138.57	0.04
	T5	876.9	2.686	40.942	0.077	84°09'	0.0046	295.6	118.00	0.04
	T6	967.9	2.86	40.691	0.077	90°00'	0	∞	123.20	0.05
	T7	1079.2	2.991	40.691	0.081	84°05'	0.0037	362.0	130.07	0.05
	T8	1248.9	2.96	40.974	0.081	78°10'	0.0082	21.7	98.41	0.06
	T9	1532.3	3.357	41.458	0.092	72°20'	0.0096	5.7	110.28	0.06
	T10	2390.3	3.616	42.225	0.068	67°02'	0.0134	**2.8**	134.60	0.05
	T11	3286.2	3.738	43.244	0.077	61°01'	0.0099	**2.6**	118.47	0.06
Span 3	T1	3541.5	2.701	55.029	0.081	61°20'	0.0211	**1.0**	121.79	0.04
	T2	3057.4	2.884	54.385	0.077	65°58'	0.0166	**2.1**	144.63	0.04
	T3	2814.4	2.792	53.954	0.077	70°19'	0.0147	4.0	137.65	0.04
	T4	2421.1	2.823	53.731	0.063	74°48'	0.0114	12.0	172.97	0.03
	T5	2089	2.747	53.709	0.068	79°12'	0.0088	37.6	160.59	0.03
	T6	1854.6	2.533	53.882	0.081	83°35'	0.0068	165.3	151.77	0.03
	T7	1533.8	2.533	54.241	0.068	87°16'	0.0028	5802.2	144.98	0.03
	T8	1354	2.335	54.777	0.068	86°37'	0.0045	1681.7	137.58	0.03
	T9	1359.2	2.319	54.777	0.063	86°37'	0.0045	1839.3	137.86	0.03
	T10	1566.7	2.548	54.241	0.063	87°16'	0.0028	6344.8	146.54	0.03
	T11	1875.1	2.518	53.882	0.077	83°35'	0.0068	180.9	152.61	0.03
	T12	2109	2.731	53.709	0.068	79°12'	0.0088	37.6	161.35	0.03
	T13	2421.1	2.838	53.731	0.063	74°48'	0.0114	12.0	172.97	0.03
	T14	2794.4	2.762	53.954	0.068	70°19'	0.0147	4.5	137.18	0.04
	T15	3067.4	2.838	54.385	0.063	65°58'	0.0166	**2.5**	144.90	0.04
	T16	3544.5	2.716	55.029	0.077	61°20'	0.0211	**1.1**	121.86	0.04
Span 4	T1	3284.8	3.738	43.244	0.063	61°01'	0.0099	3.2	118.48	0.06
	T2	2391.1	3.403	42.225	0.063	67°02'	0.0134	3.1	134.64	0.05
	T3	1513.9	-	41.458	0.077	72°20'	0.0096	7.1	109.66	0.06
	T4	1239.2	-	40.947	0.063	78°10'	0.0082	29.0	98.00	0.06
	T5	1078.5	2.869	40.691	0.077	84°05'	0.0037	396.2	130.04	0.05
	T6	967.9	3.082	40.691	0.063	90°00'	0	∞	123.24	0.05
	T7	877	2.731	40.692	0.068	85°09'	0.0046	329.2	117.30	0.05
	T8	1210.5	3.174	41.44	0.081	78°18'	0.0069	26.4	140.34	0.04
	T9	1895.8	-	42.18	0.063	72°21'	0.0083	10.8	124.92	0.06
	T10	2250.4	3.433	43.152	0.068	67°20'	0.0141	**2.7**	133.51	0.05

	T11	3194.4	3.601	44.349	0.063	66°50'	0.0132	3.5	119.88	0.06
Span 5	T1	3256.9	4.84	34.496	0.077	66°35'	0.0053	9.8	93.63	0.10
	T2	2621.7	4.747	33.392	0.068	72°21'	0.0042	27.2	111.01	0.08
	T3	2017.5	4.742	32.615	0.068	80°39'	0.0024	267.3	99.18	0.09
	T4	1542.7	4.573	32.132	0.063	90°00'	0	∞	122.33	0.07
	T5	1481.3	4.532	32.202	0.068	80°58'	0.0028	209.2	120.12	0.07
	T6	1692	4.272	32.634	0.068	73°19'	0.005	21.5	90.88	0.09
	T7	2058.4	4.242	33.412	0.068	65°48'	0.0076	5.3	98.02	0.08

APPENDIX 3. EFFECT OF CABLE LENGTH ON AXIAL CABLE FORCE

Span	Cable	[13] with l		[17]		[18]		[13] with l_e	
		T_1 (kN)	T_1/T_0	T_2 (kN)	T_2/T_0	T_3 (kN)	T_3/T_0	T_4 (kN)	T_4/T_0
Span 1	T1	2198.4	1.069	2188.2	1.064	2123.1	1.032	2057.4	1.001
	T2	1758.5	1.056	1751.0	1.051	1691.5	1.016	1642.6	0.986
	T3	1639.1	1.130	1632.5	1.125	1593.4	1.098	1530.3	1.055
	T4	1769.7	1.107	1762.8	1.103	1720.7	1.076	1654.6	1.035
	T5	1892.5	0.939	1884.2	0.935	1820.5	0.904	1763.3	0.875
	T6	2586.3	0.972	2573.6	0.967	2500.1	0.939	2411.5	0.906
	T7	3597.5	1.101	3579.3	1.096	3461.8	1.060	3357.8	1.028
Span 2	T1	3360.6	1.056	3347.9	1.052	3262.7	1.026	3192.9	1.004
	T2	2324.9	1.024	2316.4	1.021	2263.6	0.997	2206.6	0.972
	T3	1974.2	1.053	1967.6	1.049	1918.7	1.023	1872.0	0.998
	T4	1315.6	1.115	1311.5	1.111	1283.5	1.088	1246.9	1.057
	T5	905.0	1.032	902.2	1.029	877.9	1.001	856.9	0.977
	T6	1051.0	1.086	1046.1	1.081	1021.1	1.055	995.2	1.028
	T7	1112.3	1.031	1108.7	1.027	1082.1	1.003	1053.0	0.976
	T8	1301.6	1.042	1297.1	1.039	1254.7	1.005	1231.6	0.986
	T9	1724.5	1.125	1718.6	1.122	1671.5	1.091	1633.4	1.066
	T10	2585.5	1.082	2575.7	1.078	2519.4	1.054	2451.1	1.025
	T11	3500.4	1.065	3486.8	1.061	3397.9	1.034	3321.3	1.011
Span 3	T1	3746.9	1.058	3733.9	1.054	3639.5	1.028	3594.4	1.015
	T2	3317.2	1.085	3307.0	1.082	3238.4	1.059	3182.8	1.041
	T3	3055.4	1.086	3045.9	1.082	2979.0	1.058	2930.4	1.041
	T4	2568.5	1.061	2560.9	1.058	2517.1	1.040	2464.0	1.018
	T5	2428.3	1.162	2421.2	1.159	2378.3	1.138	2329.4	1.115
	T6	2073.9	1.118	2067.8	1.115	2027.8	1.093	1989.6	1.073
	T7	1695.0	1.105	1690.6	1.102	1655.2	1.079	1627.0	1.061
	T8	1466.3	1.083	1459.3	1.078	1429.5	1.056	1404.7	1.037
	T9	1445.9	1.064	1439.0	1.059	1409.5	1.037	1385.2	1.019
	T10	1715.4	1.095	1711.0	1.092	1675.4	1.069	1646.6	1.051
	T11	2049.1	1.093	2043.1	1.090	2003.2	1.068	1965.7	1.048
	T12	2399.7	1.138	2392.7	1.135	2350.0	1.114	2302.0	1.092
	T13	2596.2	1.072	2588.5	1.069	2544.5	1.051	2490.6	1.029
	T14	2989.1	1.070	2979.8	1.066	2913.5	1.043	2866.8	1.026
	T15	3210.7	1.047	3200.8	1.043	3133.1	1.021	3080.5	1.004
	T16	3789.3	1.069	3776.2	1.065	3681.4	1.039	3635.2	1.026
Span 4	T1	3500.4	1.066	3486.8	1.062	3397.9	1.034	3321.3	1.011
	T2	2285.3	0.956	2276.7	0.952	2223.1	0.930	2166.3	0.906
	T5	1021.9	0.948	1018.6	0.944	993.0	0.921	967.4	0.897
	T6	1220.5	1.261	1215.1	1.255	1188.4	1.228	1156.0	1.194
	T7	924.4	1.054	921.4	1.051	896.8	1.023	875.0	0.998
	T8	1303.0	1.076	1299.0	1.073	1271.1	1.050	1235.0	1.020
	T10	2433.2	1.081	2424.2	1.077	2370.5	1.053	2309.4	1.026
	T11	3418.3	1.070	3405.4	1.066	3319.6	1.039	3247.8	1.017
Span 5	T1	3705.4	1.138	3687.3	1.132	3572.3	1.097	3466.7	1.064
	T2	2767.3	1.056	2754.0	1.050	2680.3	1.022	2584.8	0.986
	T3	2117.9	1.050	2108.7	1.045	2042.9	1.013	1975.5	0.979
	T4	1675.5	1.086	1666.3	1.080	1627.8	1.055	1563.9	1.014
	T5	1596.4	1.078	1589.9	1.073	1550.7	1.047	1489.1	1.005
	T6	1712.7	1.012	1705.3	1.008	1645.0	0.972	1597.1	0.944
	T7	2202.3	1.070	2191.8	1.065	2124.5	1.032	2056.5	0.999